

Biom mineralization proteins: from vertebrates to bacteria

Lijun WANG (✉), Marit NILSEN-HAMILTON

Ames Laboratory, U. S. Department of Energy, Department of Biochemistry, Biophysics and Molecular Biology, Iowa State University, Ames, IA 50011, USA

© Higher Education Press and Springer-Verlag Berlin Heidelberg 2012

Abstract Biom mineralization processes are frequently found in nature. Living organisms use various strategies to create highly ordered and hierarchical mineral structures under physiologic conditions in which the temperatures and pressures are much lower than those required to form the same mineralized structures by chemical synthesis. Although the mechanism of biom mineralization remains elusive, proteins have been found responsible for the formation of such mineral structures in many cases. These proteins are active components in the process of biom mineralization. The mechanisms by which their function can vary from providing active organic matrices that control the formation of specific mineral structures to being catalysts that facilitate the crystallization of certain metal ions. This review summarizes the current understanding of the functions of several representative biom mineralization proteins from vertebrates to bacteria in the hopes of providing useful insight and guidance for further elucidation of mechanisms of biom mineralization processes in living organisms.

Keywords biom mineralization proteins, structure-function relationships, self-assembly, nanoparticles

Introduction

The term biom mineralization refers to the processes by which living organisms produce mineral structures that usually exist as pure inorganic materials in nature (Weiner, 2008). The size, morphology, composition and location of the minerals produced by living organisms are controlled by genetic factors and determined by biologic entities that are usually proteinaceous (Miller and Parker, 1984; Addadi and Weiner, 1985; Simmer and Fincham, 1995; Cha et al., 1999; Mahamid et al., 2010). Most biom mineralization processes take place under physiologic conditions where the temperatures and pressures are much lower than those required to form the same mineralized structures in the absence of organic materials. The high degree of control by biologic systems over the crystallization of inorganic elements is of interest from both the biologic and material science perspective. Although the mechanisms of biom mineralization remain elusive, results of recent investigations have begun to shed light on these fascinating processes (Gower, 2008; Weiner,

2008; Bonucci, 2009).

Minerals formed by living organisms from bacteria to vertebrates can be classified into three major categories: calcium, silicon and iron (Gower, 2008). The morphologies and structures of these biom minerals are as diverse as the living organisms that produce them. In those cases for which there is some understanding of the biologic mechanisms involved in biom mineralization, proteins have been found responsible for forming the mineral structures (Addadi and Weiner, 1985; Weiner and Addadi, 1991; Gorski, 1992; Weaver and Morse, 2003; Moradian-Oldak et al., 2006; Weiner, 2006; Weiner, 2008). The mechanisms by which mineralization proteins function are poorly understood, but they have been proposed to include the control of size, morphology, orientation, composition and the localization of crystals synthesized by organisms (Weiner, 2008; Cölfen, 2010). The role of proteins in the biom mineralization process is critical considering that biom mineralization occurs readily under mild physiologic conditions compared with the high temperatures and pressures required to produce the same products *in vitro* (Gower, 2008).

The focus of this review is to provide a brief summary of the current understanding of the functions of proteins in some selected mineralization processes of biologic systems. We will discuss the roles of collagen and amelogenin in the

Received January 4, 2012; accepted May 2, 2012

Correspondence: Lijun WANG

E-mail: wlj@iastate.edu

formation of calcium mineral (calcification) in vertebrates, the function of silicatein in the formation of silicon-based structures (silicification) in sponges and the functions of proteins, particularly Mms6, in the formation of magnetites in magnetotactic bacteria.

Collagen: an active scaffold for bone formation

Calcification and silicification are the two major systems used in nature to fabricate hard skeletal tissues (Bonucci, 2009). The calcification system in vertebrates has been studied for decades for its obvious importance for bone and tooth formation and its close relevancy to health issues. Bone contains a highly organized arrangement of apatite crystals along with the collagen fibrils (Traub et al., 1989; Hulmes et al., 1995). Collagen may be one of the most well studied fibrous proteins with its well-known triple helical three-dimensional structure (Cowan et al., 1955; Ramachandran and Kartha, 1955; Rich and Crick, 1955).

Different types of collagens have been identified in skin, bone, cartilage and blood vessels (Miller and Parker, 1984). Type I collagen, the major organic matrix found in bone, has a triple helical structure formed by two identical protein chains ($\alpha 1$) together with a third distinct one ($\alpha 2$) (Piez et al., 1961; Piez, 1965). The chains are staggered axially by 234 residues with a central triple helical region stretching about 1014 amino acids in which each chain contains glycine at every third position. Each chain has a left-handed helical structure from which a right-handed triple helical supercoil is formed (Miller and Parker, 1984). The triple helical collagen molecules self-assemble into fibrils in which molecules are axially displaced from each other by about 67 nm. There is an integral discrepancy between the displacement distance and the 300 nm length of each collagen molecule. This discrepancy results in a fibril in which some regions with cross-sections of 5 collagen molecules (overlaps) and other regions with cross-sections of 4 molecules of collagen (gaps). The gaps are believed to be the sites of calcium mineral crystallization in bone (Hodge and Petruska, 1963; Miller and Parker, 1984).

Despite the well-understood structures of collagens, the major organic matrix of the bone, studies of biomineralization during bone formation have extended for decades and yet detailed mechanisms to describe these processes still remain ambiguous (Katz and Li, 1973; Posner and Betts, 1975; Berthet-Colominas et al., 1979; Landis and Silver, 2009; Cölfen, 2010). However, the question of whether collagens provide a passive organic matrix or actively participate in the bone formation has recently been successfully addressed (Dey et al., 2010; Nudelman et al., 2010). The presence of other macromolecules in the system such as glycosaminoglycans, proteoglycans and glycoproteins, which have been speculated as either nucleators or inhibitors of calcium

mineralization in bone, complicate the problem of deciphering the mechanism of bone formation (Berthet-Colominas et al., 1979; Miller and Parker, 1984). Consequently, the key question regarding calcium mineralization in bone, which is whether the bone is mineralized by means of a classical crystallization process (nucleation and growth) or is initiated from amorphous precursors, has been debated for decades (Glimcher, 1959; Termine and Posner, 1966; Wheeler and Lewis, 1977; Glimcher et al., 1981; Weiner, 2006; Grynpas and Omelon, 2007; Olszta et al., 2007; Cölfen, 2010; Mahamid et al., 2010). In this review, we will focus on the role of the collagen matrix on calcium mineralization in the process of bone formation, although other non-collagenous proteins (including osteonectin, osteocalcin, phosphophoryn, and bone sialoprotein, etc.) are also thought to be key contributors to bone formation (Termine et al., 1981; Addadi and Weiner, 1985; Weiner and Addadi, 1991; Gorski, 1992).

Dey et al. (2010) studied biomineralization *in vitro* using an arachidic acid monolayer system to mimic the *in vivo* biologic surfaces that induce calcium phosphate biomineralization. By using cryo-TEM (transmission electron microscopy), the investigators provided high resolution, time-resolved images of the surface-induced calcium phosphate crystallization. The authors reported the existence of small nanometer-sized prenucleation clusters in the concentrated calcium solution in which the biomineralization of calcium phosphate begins. These prenucleation clusters then aggregate and further coalesce on the surface of monolayer to form amorphous spherical small particles. The development of mature crystals was accomplished by the oriented nucleation of amorphous particles directed by the monolayer (Fig. 1).

Collagens are usually considered as providing a passive protein scaffold that is the structural matrix for the organization of apatite in bone biomineralization (Berthet-Colominas et al., 1979; Miller and Parker, 1984; Traub et al., 1989; Hulmes et al., 1995; Cölfen, 2010). However, the results of recent *in vitro* and *in vivo* studies have provided evidence that collagen forms an active scaffold (Dey et al., 2010; Mahamid et al., 2010; Nudelman et al., 2010). The authors used cryo-TEM and molecular modeling to investigate the electrostatic potential energy distribution of the collagen fibril. The results showed that prenucleation clusters are negatively charged loosely packed mobile structures stabilized by non-collagenous proteins for which polyaspartate was used as a substitute (Nudelman et al., 2010). Modeling of the electrostatic potential energy distribution of the collagen fibrils also revealed the existence of positively charged regions at the border of the gap and overlap zones. The authors concluded that this positively charged region can be used for mineral infiltration and electrostatic interaction, which enables the formation of a dense network of prenucleation clusters inside the collagen fibrils. These prenucleation clusters are transformed into amorphous calcium phosphates followed by transformation to hydroxyapatite and oriented as crystalline hydroxyapatite inside the

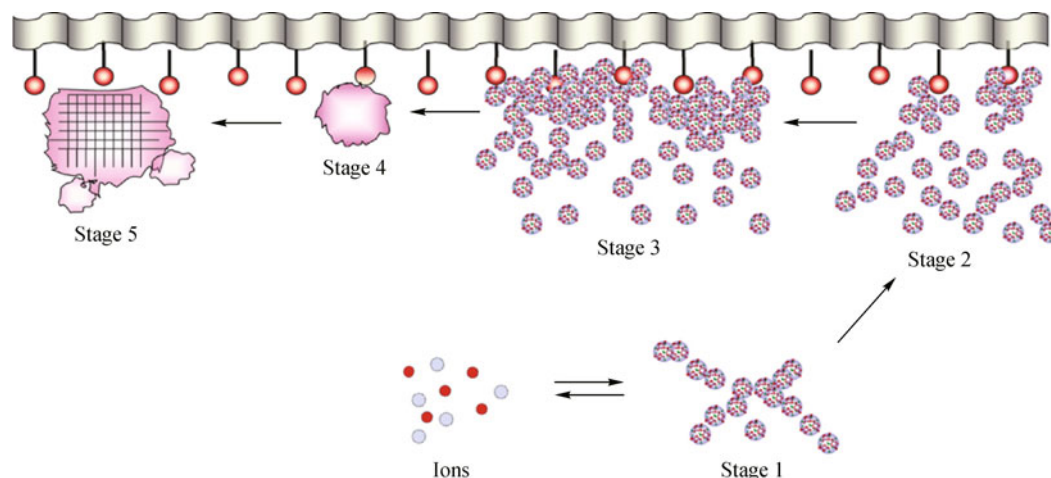


Figure 1 Schematic representation of surface-directed mineralization of calcium phosphate. Stage 1: loose aggregation of pre-nucleation clusters in equilibrium with ions in solution. Stage 2: pre-nucleation clusters aggregate in the presence of the monolayer with loose aggregates still present in solution. Stage 3: aggregation leads to densification near the monolayer. Stage 4: nucleation of amorphous spherical particles only at the monolayer surface. Stage 5: development of crystallinity following the oriented nucleation directed by the monolayer (Dey et al., 2010). Reprinted by permission from Macmillan Publishers Ltd: Nat Mater, copyright (2010).

fibrils. Thus, nucleation sites for hydroxyapatite crystallization are proposed to reside within charged amino acid domains of the collagen fibrils (Cölfen, 2010; Nudelman et al., 2010). Cryo-SEM (scanning electron microscopy) imaging and small-angle scattering also provided detailed information regarding mineral morphology and formation in the zebra fish boney fin rays for which it was concluded that packets of pre-nucleation clusters of amorphous calcium phosphates (ACP) are delivered from vesicles in the cells to the extracellular collagen matrix. These pre-nucleation clusters become fused into amorphous calcium phosphates in the collagen fibrils where maturation of the crystalline apatite then occurs (Mahamid et al., 2010).

In summary, the collagens actively participate in the formation of bone by forming a triple helical assembly with charged zones that provide the organic matrix and direct calcium deposition for bone growth.

Amelogenin: a nanospherical protein assembly responsible for enamel formation

The formation of enamel is another well-studied calcification system, which is the outcome of the mineralization of carbonated-apatite with a most unusual morphology. Mature enamel contains crystals that are tens of microns long with a length to width ratio of more than 1000 (Daculsi and Kerebel, 1978). The formation of enamel occurs extracellularly and consists of three main stages: secretory, transition and maturation (Eastoe, 1979; Simmer and Fincham, 1995). As the development of enamel continues, the extracellular matrix (ECM) proteins are cleaved by various proteases and removed from the mineralization sites in the extracellular matrix, which allows the crystals to grow in two dimensions

and increases the hardness of enamel (Eastoe, 1979; Moradian-Oldak, 2001).

Amelogenin, the major component of the extracellular matrix during the secretory stage, is believed to be responsible for the formation of the hierarchical structure in enamel (Eastoe, 1979; Moradian-Oldak, 2001). The sequences of amelogenins from different species are highly conserved at the carboxyl and N-terminal regions (Fig. 2). The C-terminal portion consists of charged hydrophilic amino acid residues and the N-terminal portion is the TRAP (tyrosine rich amelogenin polypeptide) region. The central sequence of amelogenin constitutes the hydrophobic core, which is rich in proline and leucine residues (Moradian-Oldak et al., 2000). The conserved TRAP region and the hydrophilic C-terminal region are believed to be the functional motifs important for the enamel biomineralization (Simmer and Fincham, 1995; Fincham et al., 1998).

Full length mouse amelogenin has 180 amino acids that can self-assemble *in vitro* into 'nanospheres' with hydrodynamic radii ranging from 15 to 20 nm (Fincham et al., 1994). The driving force of the self-assembly of amelogenin nanospheres seems to be hydrophobic interactions as is expected from its primary sequence that includes a large portion of hydrophobic amino acids. Amelogenin monomers form dimers, trimers and hexamers with the highly negatively charged C terminus exposed on the surface of molecule. Further self-assembly of amelogenin results in the formation of stable linear nanochains consisting of 10 to 15 linearly linked nanospheres (Aichmayer et al., 2005; Du et al., 2005a; Moradian-Oldak et al., 2006). The N- and C-terminal regions of amelogenin are susceptible to proteolytic digestion and are therefore believed to be exposed on the surface of the amelogenin nanospheres (Moradian-Oldak et al. 2001). The nanochain structure was initially reported to be birefringent with regular periodicity

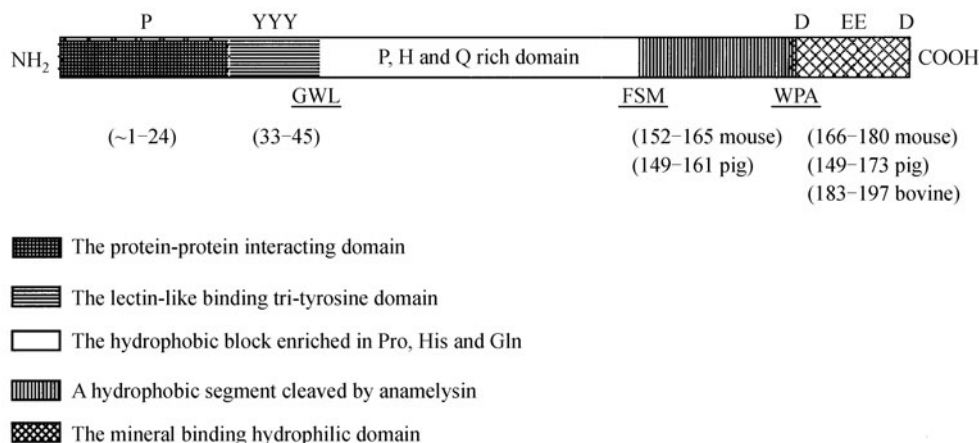


Figure 2 Schematic representation of amelogenin. Schematic presentation of some structural features of amelogenin protein based on previous reports and recent studies on self-assembly and limited proteolysis experiments. Numbers in parentheses refer to amino acids in amelogenin sequences in different species. Proteolytic activities by enamelysin occur at the GWL, FSM and WPA sites. The molecules contain one phosphorylated serine at position 16. When the absence of the hydrophilic C-terminal domain mineral binding domain, causes fusion of amelogenin nanospheres, the absence of the hydrophobic segment between FSM and WPA locus results in the formation of small nanospheres and fusion does not occur (Moradian-Oldak 2001). Reprinted with permission from Elsevier, copyright (2001).

and termed as ‘microribbon’ which was subsequently found to be an artifact due to cellulose contaminants (Du et al. 2005b).

The detailed observations of the structural forms of amelogenin just described were made under bulk solution conditions which differ substantially from the *in vivo* environment where enamel is formed. *In vivo*, amelogenin is very likely to interact with charged biologic surfaces of other proteins, lipids or mineral crystals. However, a similar quaternary structure of amelogenin was observed *in vivo* by high resolution TEM as observed *in vitro*. In TEM images of developing enamel in mouse, bovine and hamster, the amelogenin nanospheres appear as ‘beaded rows’ aligned with and separating the enamel crystallites (Fincham et al., 1995). The nanosphere structure of amelogenin was proposed to control the spacing of initial crystallite, which is found to be about 20 nm in developing mouse enamel (Diekwisch et al., 1995; Fincham et al., 1995; Zeichner-David et al., 1995).

The C-terminal region of amelogenin participates in forming its higher order quaternary structures. Nanospheres of amelogenin lacking this domain are more loosely organized and larger than those formed by the full length amelogenin (Moradian-Oldak et al., 2002). The C-terminal domain deletion mutant also fails to form nanochains (Du et al., 2005a; Moradian-Oldak et al., 2006). In the absence of the highly negatively charged C-terminal domain, amelogenin has a much lower affinity for apatite crystals (Moradian-Oldak et al., 2002). This result is supported by the results of a solid-state nuclear resonance microscopy (SSNMR) study of leucine-rich amelogenin protein (LRAP), the product of an alternatively spliced product of the primary amelogenin transcript, showing the C-terminal domain oriented to the surface of hydroxyapatite (HAP) with the acidic amino acid

residues in the C-terminal domain in position to directly interact with the HAP surface and regulate mineralization (Shaw et al., 2004).

The shapes of the hydroxyapatite crystals of enamel are highly asymmetric (about 26 nm in thickness, 68 nm in width and more than 1 mm in length for human enamel) (Daculsi and Kerebel, 1978). The means by which this shape might be generated by amelogenin was investigated by single-molecule AFM (atomic force microscopy) studies that demonstrated face-specific adsorption to hydroxyapatite crystals of an amelogenin fragment consisting of the C-terminal 12 amino acids (Friddle et al., 2011). It is proposed that amelogenin controls elongation of HAP along the (001) face by selectively binding to and inhibiting crystal growth at the (100) face. The C-terminal fragment of amelogenin preferentially binds to calcium ions at the (100) surface of hydroxyapatite (HAP) crystals with a high affinity comparable to that for the interaction between biotin and streptavidin. This strong interaction can be attributed to the binding of Ca^{2+} by the negatively charged carboxylate groups in the C-terminal fragment of amelogenin that are predicted by molecular dynamics simulations of the peptide-apatite complex to lie flat on the (100) surface of hydroxyapatite (Friddle et al., 2011).

Another aspect that influences biomineralization *in vivo* is the nature of the surface on which the activity occurs. Recent *in situ* studies of the effects of different charged surfaces on amelogenin assembly revealed complex charge and substrate dependent pathways and patterns of amelogenin self-assembly that differ from those in bulk solution (Tarasevich et al., 2009; Tarasevich et al., 2010; Chen et al., 2011). For example, when exposed to the positively charged 3-aminopropyl triethoxysilane (APS) silanized mica, amelo-

genin initially self-assembled into decamers, which either further assembled into higher-order structures or dissociated into monomers. Negatively charged bare mica surfaces promoted the formation of a film of amelogenin monomers that interacted with weak affinity. Thus, the quaternary structure of amelogenin *in vivo* may vary depending on the charge of the surface with which it interacts. As both types of surfaces (positively or negatively charged) are commonly present during amelogenin-controlled enamel formation, all the amelogenin structures observed *in vitro* may have biologic relevance for enamel formation: the monomeric and oligomeric forms of amelogenin may control growth and morphology of the crystals, while the higher-order structures (nanospheres, nanochains) may dictate the spacing and organization of the mineral crystals (Tarasevich et al., 2009; Tarasevich et al., 2010; Chen et al., 2011).

Briefly, the amelogenin self-assembles into high-order structures to control the spacing of initial crystallite during enamel development, while the specific binding of amelogenin to a certain mineral face is the key factor that determines the morphology of the hydroxyapatite crystals in enamel.

Silicatein: a dehydrogenase that catalyzes silicon condensation

Silicification is another biom mineralization process frequently used by organisms to fabricate silica-based hard structures such as diatom walls, sponge spicules and radiolarian microskeletons (Crookes-Goodson et al., 2008; Bonucci, 2009). Diatoms exist in almost every aquatic habitat and are believed to play critical roles in global carbon fixation (Dugdale and Wilkerson, 1998; Sumper and Brunner, 2006). More than 10000 species of diatoms have been identified based on the morphology and structure of their cell walls (Sumper and Brunner, 2006). The formation of these silica-based nanostructures is under strict genetic control (Sumper and Brunner, 2006; Hildebrand, 2008; Kröger and Poulsen, 2008). It is a formidable task to reproduce these highly organized hierarchical nano- and microstructures that are routinely assembled by diatoms, sponges and radiolarians (Tacke, 1999; Falciatore and Bowler, 2002; Hildebrand, 2003; Brutchey and Morse, 2008). The capabilities of these organisms are even more impressive considering that biologic silicification occurs under physiologic conditions, while the *in vitro* synthesis of silica usually involves high temperature and/or extreme pH (Stöber et al., 1968; Brinker and Scherrer, 1990). A number of articles reviewing the roles of proteins isolated from diatoms and sponges involved in silicification have been published during the past several years (Brutchey and Morse, 2008; Hildebrand, 2008; Kröger and Poulsen, 2008; Brunner et al., 2009). In this review, we will use silicatein as an example to briefly discuss the functions of protein in the process of silicification.

The skeletons (or spicules) of sponges are built of hydrated amorphous silica with the shapes varying between species (Simpson, 1984; Levi et al., 1989). The spicules are robust structures of amorphous silica consisting of annular layers of silica nanoparticles surrounding a central proteinaceous axial filament (Weaver and Morse, 2003; Crookes-Goodson et al., 2008). It is believed that this proteinaceous filament is assembled by constituent protein subunits. The deposition of silica occurs in the space between the proteinaceous filament and sclerocyte membrane and is under the control of proteinaceous filament with the participation of some small peptides and polyamines (Pascal et al., 2005; Matsunaga et al., 2007; Brutchey and Morse, 2008).

Silicatein, the major component of the central proteinaceous axial filaments of sponges, was first identified from the marine demosponge *Tethya aurantia* (Shimizu et al., 1998). The silicatein filaments are composed by three subunits, silicatein α , β and γ , with the approximate molar ratio of being 12 : 6 : 1 (α : β : γ). All of the three subunits share high degree of similarity in terms of amino acid compositions and isoelectric point (Shimizu et al., 1998). The fact that only the genes of silicatein α and β have been found in marine demosponges suggests that the γ subunit may be a post-translational product of either α or β subunits (Shimizu et al., 1998; Krasko et al., 2002). Silicatein isoforms from several species of marine and freshwater demosponges share a high degree of similarity with the silicatein isolated from *T. aurantia* (Krasko et al., 2000; Pozzolini et al., 2004; Schröder et al., 2004a; Schröder et al., 2004b; Kaluzhnaya et al., 2007).

The first function of silicatein is to self-assemble into filaments that template silica deposition (Shimizu et al., 1998). The process of silicatein self-assembly appears to be through fractal intermediates (Fig. 3). The silicatein monomers first form stable oligomers (dimers, trimers and tetramers) through intermolecular disulfide bonds that subsequently assemble into fractal intermediate structures. These fractal intermediate structures are further condensed and organized into ordered filamentous structures (Murr and Morse, 2005). The fractal intermediates in the self-assembly of silicatein filaments were first observed in the demosponge *Tethya aurantia* and confirmed in the demosponge *Suberites domuncula* (Müller et al., 2007). These observations suggest that the spontaneous organization of silicatein filaments through fractal intermediates may be a general mechanism in sponges.

The second function of silicatein in the process of silicification in sponges is to act as a dehydrogenase for silicon ethoxide condensation (Cha et al., 1999; Zhou et al., 1999). Silicatein shares high sequence homology to human cathepsin L, which is a cysteine protease, with two of the three amino acids of the catalytic triad of cathepsins, His and Asn, conserved in silicatein (Shimizu et al., 1998). The mechanism of silicatein-catalyzed polymerization of silica is proposed to resemble the catalytic mechanism of a serine protease. The dehydration of silicon ethoxide promoted by silicateins and

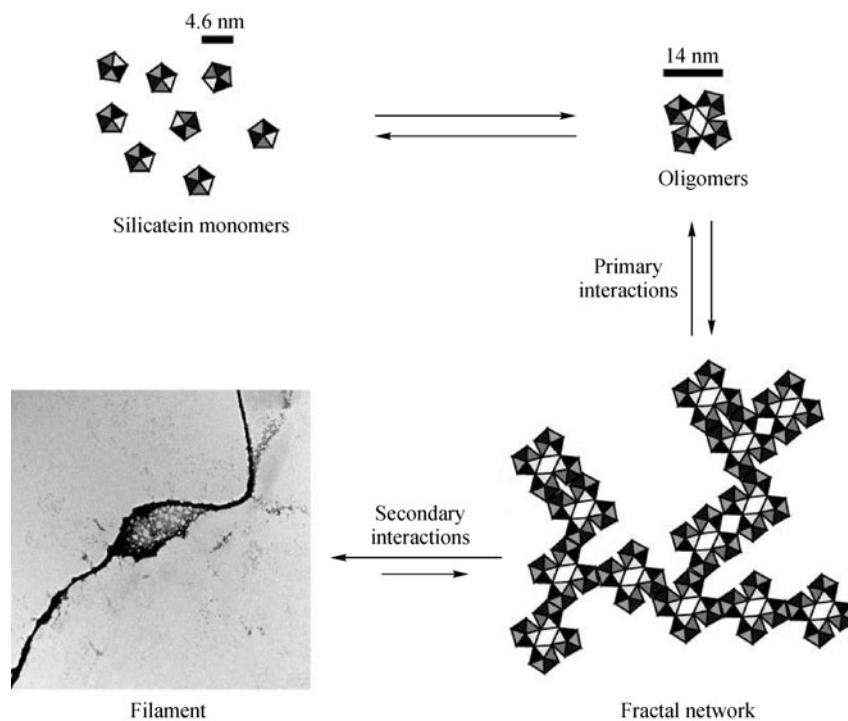


Figure 3 Model of the fractal assembly of silicatein. Silicatein monomers associate into oligomers via disulfide bonds. The oligomers form fractal networks by diffusion-limited aggregation. As soon as the fractal network is formed, the close proximity and reduction in degrees of freedom drives the condensation and organization into a filament (Murr and Morse 2005). Reprinted with permission from National Academy of Sciences, copyright (2005).

the cleavage of peptides catalyzed by serine proteases both proceed through an obligatory hydrolysis reaction and both are accelerated by general acid-base catalysis (Fig. 4). The dehydrolase activity of silicatein was first demonstrated *in vitro* by using tetraethyl orthosilicate (TEOS) as the substrate. The hydrolysis of TEOS at room temperature and neutral pH was only observed in the presence of silicatein (Cha et al., 1999). Later site-directed mutagenesis studies further demonstrated that the His and Ser residues of the catalytic center of silicatein are required for its activity (Zhou et al., 1999).

Research into the activities of silicatein in the process of silicification has revealed a dual function for silicatein, which is both a hydrolytic enzyme and a template for biosilicification. The elucidation of the mechanism of silicatein-directed biosilicification has inspired the invention of new route to fabricate new nano- and microstructured materials (Brutchey and Morse, 2006; Kisailus et al., 2006; Brutchey et al., 2008; Brutchey and Morse, 2008; Rabuffetti et al., 2012).

Mms6: a protein micelle that promotes magnetic nanoparticle formation *in vitro*

Magnetotactic bacteria are the most ancient and simplest organisms capable of performing mineralization. They are aquatic prokaryotes equipped with flagella and move under the direction of local geomagnetic field lines (Blakemore, 1975). All magnetotactic bacteria have unique intracellular

structures, called magnetosomes that consist of magnetic nanoparticles surrounded by lipid bilayer membranes (Balkwill et al., 1980; Ofer et al., 1984; Gorby et al., 1988). The magnetosomes are found arranged in a single string of one or more chains, which is believed to be the physical basis of the magnetotactic trait (Penninga et al., 1995; Dunin-Borkowski et al., 1998; Bazylinski and Frankel, 2004). The chain(s), positionally fixed in the cell, act as tiny compasses to guide bacterial migration along local geomagnetic field lines. Magnetotaxis is proposed to simplify the bacterial search for the optimal microaerobic environment to a one-dimensional rather than a random three dimensional path (Blakemore, 1975; Frankel et al., 1997; Bazylinski and Frankel, 2004; Komeili, 2007).

Despite the apparent simplicity of the model system, reports of studies of biomineralization in magnetotactic bacteria have been infrequent. Magnetotactic bacteria are very sensitive to the environmental oxygen concentration for their growth and magnetosome synthesis. Their fastidious requirements for a very narrow range of low oxygen concentrations have limited the progress in this research field for many years and the number of pure cultured strains is still very small (Blakemore et al., 1979; Frankel et al., 1979; Bazylinski and Frankel, 2004). However, after the genomes of several magnetotactic bacteria were sequenced and annotated, investigation of the molecular mechanisms of magnetosome formation became possible due to the identi-

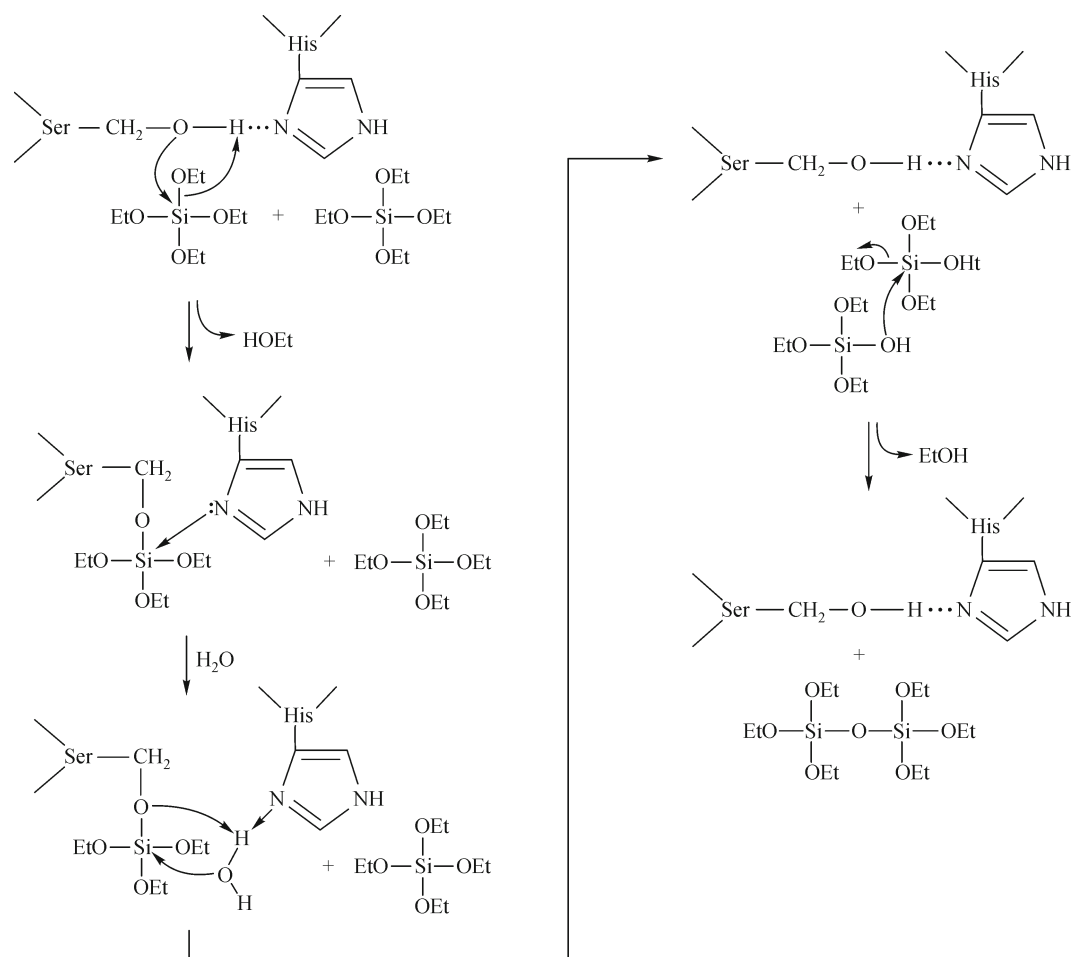


Figure 4 Mechanism of silicatein catalyzed condensation of silicon ethoxide. Proposed reaction mechanism of silicon ethoxide condensation catalyzed by silicatein α , based on the well characterized mechanism of catalysis by the Ser/His and Cys/His active-site proteases. R = phenyl- or methyl- for the silicon triethoxide substrates, and R = $\text{CH}_3\text{CH}_2\text{—O—}$ (= EtO—) for TEOS. Hydrogen-bonding between the imidazole nitrogen of the conserved histidine and the hydroxyl of the active-site serine is proposed to increase the nucleophilicity of the serine oxygen, potentiating its attack on the silicon atom of the substrate. Nucleophilic attack on the silicon displaces ethanol, forming a covalent protein—O—Si intermediate (potentially stabilized as the pentavalent silicon adduct via donor bond formation with the imidazole nitrogen). The addition of water completes hydrolysis of the first alkoxide bond. Condensation initiated by nucleophilic attack of the released Si—O— on the silicon of the second substrate molecule then forms the disiloxane product (Cha et al. 1999). Reprinted with permission from National Academy of Sciences, copyright (1999).

fication of potential biom mineralization proteins that can be expressed *in vitro* (Richter et al., 2007).

Although generally believed to be only a feature of eukaryotes, intracellular compartments are found in many bacterial strains. One example is the magnetosome, which is an invagination of the magnetotactic bacterial cell cytoplasmic membrane (Murat et al., 2010a). Although never fully separated from their membrane source, magnetosomes are vesicles, each containing a magnetic nanoparticle (usually 35 to 120 nm in diameter) and surrounded by a lipid bilayer membrane with similar composition as the cytoplasmic membrane (Balkwill et al., 1980; Bazylinski and Frankel, 2004; Komeili, 2007). These vesicles are organized into chains by cytoskeletal filaments and fixed in position inside

the cells (Komeili, 2007).

The means by which iron is taken up and the magnetite crystal develops in the magnetosome was investigated in a systematic study of the magnetite biom mineralization pathway in *Magnetospirillum gryphiswaldense* strain MSR-1. The results showed that iron is taken up from the environment through the cytoplasmic membrane either in the ferric or ferrous form (Faivre et al., 2007). These investigators report that ferric iron is chelated by some unknown organic substrate associated with the membrane, while ferrous iron is sequestered by membrane-associated bacterial ferritin. The ferric and ferrous ions are transported directly into the invaginated magnetosome vesicles without passing through the cytoplasm and magnetite formation is initiated by rapid

coprecipitation of ferric and ferrous ions without any precursor phase. However, another study of the formation of magnetosome in *Magnetospirillum gryphiswaldense* strain MSR-1 using real-time X-ray magnetic circular dichroism, showed contradictory results (Staniland et al., 2007). These investigators reported the formation of full size nanocrystals with nonmagnetic surface layers constituted by hematite (the nonmagnetic precursor of magnetite) within 15 min of initiation of magnetosome particle formation. The transformation of hematite to mature magnetite nanoparticles was completed within another 15 min. The fact that bacteria only took 30 min to synthesize the magnetites suggests that this process may be catalytic as proposed by the authors.

Genomic and proteomic studies of *Magnetospirillum magneticum* AMB-1 have identified 48 magnetosome-associated proteins (Matsunaga et al., 2005). The mature Mms6 is a 59 amino acid protein with hydrophobic amino acids concentrated in the N-terminal half and hydrophilic amino acids in the C-terminal half (Fig. 5A). It was first reported as a magnetosome membrane-associated protein isolated with magnetite nanoparticles from the *Magnetospirillum magneticum* strain AMB-1 (Arakaki et al., 2003). In their report, Arakaki et al. identified several small proteins, Mms5, Mms6, Mms7 and Mms13 that were tightly bound to the bacterial synthesized magnetite nanoparticles. Only Mms6 was reported to promote the formation of magnetite nanoparticles with similar morphology to bacterial magnetites *in vitro* by co-precipitation of ferric and ferrous ion (Arakaki et al., 2003). Magnetization measurements and transmission electron microscopy of magnetite nanoparticles synthesized in the presence of recombinant Mms6 further verified the protein's function in controlling the size and morphology of magnetite nanoparticles during *in vitro* synthesis (Prozorov et al., 2007a).

Cubo-octahedral magnetite nanoparticles are formed by partial oxidation of ferrous hydroxide in the presence of Mms6 compared to octahedral magnetites with broad size distribution in its absence. It was proposed that Mms6 controls the morphology of magnetites during their *in vitro* growth by binding a specific crystal face (Amemiya et al., 2007).

Mms6 or its C-terminal domain covalently linked to self-assembling polymers can also promote the synthesis of cobalt ferrite nanoparticles, a mineral form not known to be present in any living organism. The cobalt ferrite nanocrystals produced in the presence of Mms6 exhibited 50–80 nm thin hexagon-like structures that are difficult to produce using conventional techniques (Prozorov et al., 2007b).

In the *Magnetospirillum magneticum* strain AMB-1 deletion mutant of the *mms6* gene ($\Delta mms6$), only smaller size bacterial magnetites with uncommon crystal faces were observed (Tanaka et al., 2011). The complementation strains of $\Delta mms6$ mutant synthesized magnetites similar to those in the wild type with uniformed cubo-octahedral morphology (Tanaka et al., 2011). Deletion of the *mms6* gene also resulted

in a significant decrease of the levels of Mms5, Mms7, and Mms13 on the surfaces of bacterial magnetites. Thus, it was proposed that Mms6 may serve as a scaffold protein, forming a complex with other Mms proteins that co-localizes these proteins onto the bacterial magnetite surface and thereby controls the morphology and size of these nanoparticles.

The N-terminal domain of Mms6 contains a Leu-Gly-rich region, which is similar to that of some self-aggregating proteins of other biomineralization systems (Amemiya et al., 2007; Komeili, 2007; Faivre and Schüler, 2008; Schüler, 2008). Consistent with this observation, Mms6 self-assembles into water-soluble protein micelles. The hydrophobic N-terminal domain of Mms6 anchors the hydrophilic C-terminal domain in the micelle from which the latter binds iron and promotes the nucleation and growth of magnetite nanoparticles. The ability of Mms6 to self-assemble allows it to form an extended surface of C-terminal domains that could template the crystallization of magnetite (Wang et al., 2012a).

The hydrophilic C-terminal domain of Mms6 contains a series of amino acid residues with either hydroxyl or carboxyl groups (serine, aspartate or glutamate). It has been speculated that these residues may provide a template for magnetic nanoparticle synthesis and can control the morphology of the magnetite (Arakaki et al., 2003). Quantitative iron binding studies show that Mms6 binds one Fe^{3+} with a very high affinity ($K_d = 10^{-16}$ M) at pH 7 which can be attributed to the C-terminal domain. At pH 3, the *in vitro* condition used for iron crystal formation by this protein, Mms6 exhibits two binding phases with respect to iron concentration (Fig. 5B). The first phase is stoichiometric with respect to iron and high affinity. The second phase shows cooperative iron binding (Hill n value ~ 3) with high capacity (~ 20 iron molecules per Mms6 molecule). The high affinity stoichiometric binding has been proposed to contribute to the C-terminal domain adopting an appropriate conformation, whereas the second low affinity iron binding phase in which iron clusters on the protein cooperatively and at high stoichiometry is consistent with crystal building. The cooperativity suggests that the protein organizes the iron on its surface in groups of three iron atoms which might reflect packing into the magnetite crystal lattice for which the minimal unit is a triad of two Fe^{3+} and one Fe^{2+} (Wang et al., 2012a).

The micellar structure of Mms6 also enables it to form a stable monomolecular layer at the aqueous-vapor interface. By using X-ray reflectivity and surface fluorescence spectroscopy it was demonstrated that, at low pH, the Mms6 monolayer can bind to Fe^{3+} with a much higher affinity than to Fe^{2+} (Wang et al., 2012b).

Another interesting aspect of the binding properties of Mms6 to iron is the difference in affinity between pH 3 and pH 7.5. The authors attributed this to structural changes that Mms6 undergoes in the shift from lower to higher pH, the evidence of which can be found from the CD spectrum (Wang et al., 2012a). The *in vitro* synthesis of Mms6-promoted formation of magnetite nanoparticles involves a pH change

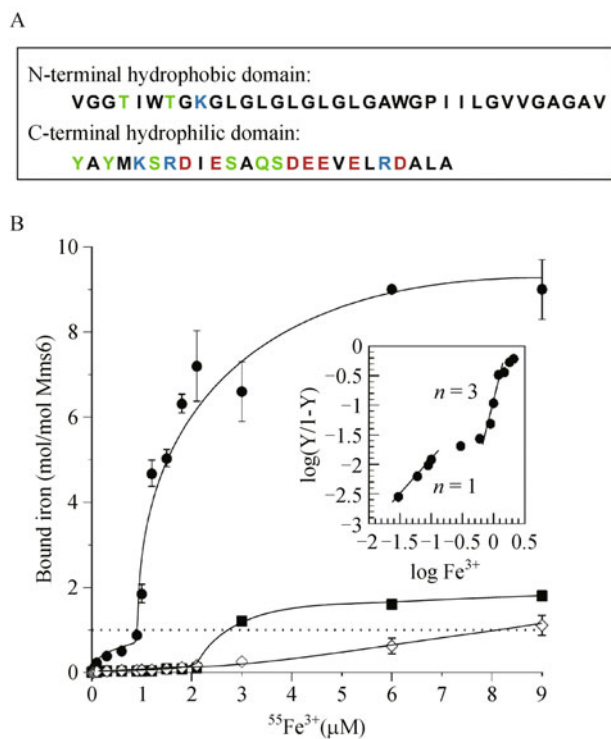


Figure 5 Mms6, an iron-binding protein that forms magnetic nanoparticles. (A) Sequence of mature Mms6. Acidic amino acid residues are colored in red, basic amino acid residues are colored in blue and polar uncharged amino acid residues are colored in green. (B) Two phases of iron binding by Mms6. Binding of Mms6 to free ferric iron was measured using $^{55}\text{FeCl}_3$ with the filter assay at pH 3. Inset: Hill plot. ●: Mms6, ◇, ■: Control proteins (Wang et al. 2012a). Reprinted with permission from American Chemical Society, copyright (2012).

from acidic to basic by the addition of NaOH to a low pH solution containing Mms6 (Prozorov et al., 2007a). Similarly, the process of magnetite formation in magnetosomes has been proposed to be coordinated with an increase in pH, starting with a low pH required for the accumulation of a high concentration of iron and eventually reaching a basic pH necessary for the maturation and stability of magnetites (Wang et al., 2012a).

Magnetites (Fe_3O_4) are stable only in alkaline environments ($\text{pH} > 7$), while hematite (Fe_2O_3), the non-magnetic precursor of magnetites, can be stable from pH 1 to pH 14 (Bell et al., 1987). Although the existence of the precursor during magnetite formation in magnetotactic bacteria is still under debate (Faivre et al., 2007; Staniland et al., 2007), there is some evidence in favor of the hypothesis that the pH inside magnetosomes may change during magnetite formation. For instance, the results of recent studies of MamM and MamB (two putative cation diffusion facilitators) from *Magnetospirillum gryphiswaldense* indicate that H^+ transporters may be involved in controlling the magnetite growth in magnetosomes (Nies, 2011; Uebe et al., 2011). Other evidence for a

pH change during magnetite growth *in vivo* comes from studies of the deletion mutant of the *mamN* gene (*ΔmamN*) in *Magnetospirillum magneticum* strain AMB-1 (Murat et al., 2010a). The MamN protein has been proposed as a putative homolog of the Na^+/H^+ antiporter and therefore may regulate pH inside magnetosome vesicles during magnetite formation (Murat et al., 2010b; Komeili, 2012). The *Magnetospirillum magneticum ΔmamN* mutant failed to synthesize magnetites but empty and intact magnetosomes were observed. It will be of interest to investigate possible pH changes in magnetosomes during the formation of magnetites to further understand the mechanism of magnetite formation in magnetotactic bacteria.

It has been proposed that the formation of larger particles can be achieved by the fusion of smaller particles via coalescence when these smaller particles can move, collide and combine (Thiel et al., 2009; Evans and Thiel, 2010). A recent *in situ* high resolution TEM study of the formation of platinum nanoparticle in graphene liquid cell provided direct visual evidence for the above hypothesis (Yuk et al., 2012). The micellar structure and high capacity iron binding observed for Mms6 may provide some insights toward the further elucidation of the mechanism of magnetite formation in magnetotactic bacteria. Mms6 is very likely to be mobile in the magnetosome membrane and perhaps move as small protein islands. The high capacity binding of iron for Mms6 may reflect the initiation of crystal seeds. Together with its ability to bind iron at high stoichiometry, the mobility of Mms6 in the micelle or magnetosome membrane may promote the fusion of crystal seeds into larger magnetic nanoparticles.

Concluding remarks

Living organisms use different strategies to create highly ordered and hierarchical mineral structures with fundamental structural elements at nanometer scales. The ability to fabricate such fundamental structures independently of these organisms could open many new and exciting opportunities in nanotechnology. Proteins, the organic phase in many of the biomineralization systems, play critical roles in the formation of such structures. The biomineralization proteins from different biologic systems discussed here are not just passive matrices for mineral deposition but are actively involving in the mineralization process. They also all undergo a process of self-assembly, but in different patterns that may influence the structure of their crystalline mineral products. The dense triple helical assembly of collagens is important for building bone structure with its strong mechanical property. The amelogenin nanospheres and nanochains control the spacing and organization of the hydroxyapatite crystals that form the enamel structure. The fractal assembly pattern observed in silicatein filaments seems to be related to the sophisticated patterns of the silica-based

structures that sponges fabricate. Although there is limited information regarding the function of Mms6 in the process of magnetite formation *in vivo*, the micellar structures that Mms6 forms *in vitro* may reflect a protein assembly *in vivo* that enables iron crystallization on a surface of repeated iron binding domains and also provides for a mobility of protein islands in the membrane favorable for the fusion of small crystal seeds into larger magnetite nanoparticles.

The study of biomineralization is fundamentally in the realm of structure: the structures of the organic phases (usually proteins), the inorganic phases (mineral component) and particularly the interface between organic and inorganic phases (Weiner, 2008). Biomineralization proteins usually self-assemble into higher order supramolecular structures that are critical for controlling the mineral phase deposition and structure. Such large protein assemblies are usually not amenable to conventional biophysics approaches, such as X-ray crystallography or solution NMR spectroscopy, for the investigation of their 3D structures. However, as discussed here, significant progress in the understanding of the mechanism of action of biomineralization proteins can come from biophysical analyses, such as solid state NMR, electron microscopy, AFM, atomistic and coarse grain computational simulations, combined with biochemical, genetic and functional analysis. The convergence of these multidisciplinary approaches will surely continue to be the means of understanding the variety of structures and functions of biomineralization proteins and how they interact with the inorganic phases that they control.

Further understanding of the principles of biomineralization is obviously of great interest to the development of more refined methods for fabricating new bioinspired materials. Such goals will not be accomplished without the close collaboration between a variety of disciplines such as molecular biology, chemistry, physics, material science and engineering.

References

- Addadi L, Weiner S (1985). Interactions between acidic proteins and crystals: stereochemical requirements in biomineralization. *Proc Natl Acad Sci USA*, 82(12): 4110–4114
- Aichmayer B, Margolis H C, Sigel R, Yamakoshi Y, Simmer J P, Fratzl P (2005). The onset of amelogenin nanosphere aggregation studied by small-angle X-ray scattering and dynamic light scattering. *J Struct Biol*, 151(3): 239–249
- Amemiya Y, Arakaki A, Staniland S S, Tanaka T, Matsunaga T (2007). Controlled formation of magnetite crystal by partial oxidation of ferrous hydroxide in the presence of recombinant magnetotactic bacterial protein Mms6. *Biomaterials*, 28(35): 5381–5389
- Arakaki A, Webb J, Matsunaga T (2003). A novel protein tightly bound to bacterial magnetic particles in *Magnetospirillum magneticum* strain AMB-1. *J Biol Chem*, 278(10): 8745–8750
- Balkwill D L, Maratea D, Blakemore R P (1980). Ultrastructure of a magnetotactic spirillum. *J Bacteriol*, 141(3): 1399–1408
- Bazylinski D A, Frankel R B (2004). Magnetosome formation in prokaryotes. *Nat Rev Microbiol*, 2(3): 217–230
- Bell P E, Mills A L, Herman J S (1987). Biogeochemical conditions favoring magnetite formation during anaerobic iron reduction. *Appl Environ Microbiol*, 53(11): 2610–2616
- Berthet-Colominas C, Miller A, White S W (1979). Structural study of the calcifying collagen in turkey leg tendons. *J Mol Biol*, 134(3): 431–445
- Blakemore R (1975). Magnetotactic bacteria. *Science*, 190(4212): 377–379
- Blakemore R P, Maratea D, Wolfe R S (1979). Isolation and pure culture of a freshwater magnetic spirillum in chemically defined medium. *J Bacteriol*, 140(2): 720–729
- Bonucci E (2009). Calcification and silicification: a comparative survey of the early stages of biomineralization. *J Bone Miner Metab*, 27(3): 255–264
- Brinker C J, Scherrer G W (1990). *Sol-gel science: the chemistry of sol-gel processing*. New York: Academic Press
- Brunner E, Gröger C, Lutz K, Richthammer P, Spinde K, Sumper M (2009). Analytical studies of silica biomineralization: towards an understanding of silica processing by diatoms. *Appl Microbiol Biotechnol*, 84(4): 607–616
- Brutchey R L, Cheng G, Gu Q, Morse D E (2008). Positive temperature coefficient of resistivity in donor-doped BaTiO₃ ceramics derived from nanocrystals synthesized at low temperature. *Adv Mater*, 20(5): 1029–1033
- Brutchey R L, Morse D E (2006). Template-free, low-temperature synthesis of crystalline barium titanate nanoparticles under bio-inspired conditions. *Angew Chem Int Ed Engl*, 45(39): 6564–6566
- Brutchey R L, Morse D E (2008). Silicatein and the translation of its molecular mechanism of biosilicification into low temperature nanomaterial synthesis. *Chem Rev*, 108(11): 4915–4934
- Cha J N, Shimizu K, Zhou Y, Christiansen S C, Chmelka B F, Stucky G D, Morse D E (1999). Silicatein filaments and subunits from a marine sponge direct the polymerization of silica and silicones *in vitro*. *Proc Natl Acad Sci USA*, 96(2): 361–365
- Chen C L, Bromley K M, Moradian-Oldak J, DeYoreo J J (2011). In situ AFM study of amelogenin assembly and disassembly dynamics on charged surfaces provides insights on matrix protein self-assembly. *J Am Chem Soc*, 133(43): 17406–17413
- Cölfen H (2010). Biomineralization: A crystal-clear view. *Nat Mater*, 9(12): 960–961
- Cowan P M, McGavin S, North A C T (1955). The polypeptide chain configuration of collagen. *Nature*, 176(4492): 1062–1064
- Crookes-Goodson W J, Slocik J M, Naik R R (2008). Bio-directed synthesis and assembly of nanomaterials. *Chem Soc Rev*, 37(11): 2403–2412
- Daculus G, Kerebel B (1978). High-resolution electron microscope study of human enamel crystallites: size, shape, and growth. *J Ultrastruct Res*, 65(2): 163–172
- Dey A, Bomans P H H, Müller F A, Will J, Frederik P M, de With G, Sommerdijk N A J M (2010). The role of prenucleation clusters in surface-induced calcium phosphate crystallization. *Nat Mater*, 9(12): 1010–1014
- Diekwich T G H, Berman B J, Gentner S, Slavkin H C (1995). Initial enamel crystals are not spatially associated with mineralized dentine.

- Cell Tissue Res, 279(1): 149–167
- Du C, Falini G, Fermani S, Abbott C, Moradian-Oldak J (2005a). Corrections and clarifications. *Science*, 309(5744): 2166
- Du C, Falini G, Fermani S, Abbott C, Moradian-Oldak J (2005b). Supramolecular assembly of amelogenin nanospheres into birefringent microribbons. *Science*, 307(5714): 1450–1454
- Dugdale R C, Wilkerson F P (1998). Silicate regulation of new production in the equatorial Pacific upwelling. *Nature*, 391(6664): 270–273
- Dunin-Borkowski R E, McCartney M R, Frankel R B, Bazylinski D A, Pósfai M, Buseck P R (1998). Magnetic microstructure of magnetotactic bacteria by electron holography. *Science*, 282(5395): 1868–1870
- Eastoe J E (1979). Enamel protein chemistry—past, present and future. *J Dent Res*, 58(Spec Issue B suppl): 753–764
- Evans J W, Thiel P A (2010). Chemistry. A little chemistry helps the big get bigger. *Science*, 330(6004): 599–600
- Favre D, Böttger L H, Matzanke B F, Schüler D (2007). Intracellular magnetite biomineralization in bacteria proceeds by a distinct pathway involving membrane-bound ferritin and an iron(II) species. *Angew Chem Int Ed Engl*, 46(44): 8495–8499
- Favre D, Schüler D (2008). Magnetotactic bacteria and magnetosomes. *Chem Rev*, 108(11): 4875–4898
- Falcatore A, Bowler C (2002). Revealing the molecular secrets of marine diatoms. *Annu Rev Plant Biol*, 53(1): 109–130
- Fincham A G, Leung W, Tan J and Moradian-Oldak J (1998). Does amelogenin nanosphere assembly proceed through intermediary-sized structures? *Connect Tissue Res*, 38(1–4): 237–240; discussion 241–236
- Fincham A G, Moradian-Oldak J, Diekwisch T G, Lyaru D M, Wright J T, Bringas P Jr, Slavkin H C (1995). Evidence for amelogenin “nanospheres” as functional components of secretory-stage enamel matrix. *J Struct Biol*, 115(1): 50–59
- Fincham A G, Moradian-Oldak J, Simmer J P, Sarte P, Lau E C, Diekwisch T, Slavkin H C (1994). Self-assembly of a recombinant amelogenin protein generates supramolecular structures. *J Struct Biol*, 112(2): 103–109
- Frankel R B, Bazylinski D A, Johnson M S, Taylor B L (1997). Magneto-aerotaxis in marine coccoid bacteria. *Biophys J*, 73(2): 994–1000
- Frankel R B, Blakemore R P, Wolfe R S (1979). Magnetite in freshwater magnetotactic bacteria. *Science*, 203(4387): 1355–1356
- Friddle R W, Battle K, Trubetskoy V, Tao J, Salter E A, Moradian-Oldak J, De Yoreo J J, Wierzbicki A (2011). Single-molecule determination of the face-specific adsorption of Amelogenin’s C-terminus on hydroxyapatite. *Angew Chem Int Ed Engl*, 50(33): 7541–7545
- Glimcher M J (1959). Molecular biology of mineralized tissues with particular reference to bone. *Rev Mod Phys*, 31(2): 359–393
- Glimcher M J, Bonar L C, Grynblas M D, Landis W J, Roufosse A H (1981). Recent studies of bone mineral: Is the amorphous calcium phosphate theory valid? *J Cryst Growth*, 53(1): 100–119
- Gorby Y A, Beveridge T J, Blakemore R P (1988). Characterization of the bacterial magnetosome membrane. *J Bacteriol*, 170(2): 834–841
- Gorski J P (1992). Acidic phosphoproteins from bone matrix: a structural rationalization of their role in biomineralization. *Calcif Tissue Int*, 50(5): 391–396
- Gower L B (2008). Biomimetic model systems for investigating the amorphous precursor pathway and its role in biomineralization. *Chem Rev*, 108(11): 4551–4627
- Grynblas M D, Omelon S (2007). Transient precursor strategy or very small biological apatite crystals? *Bone*, 41(2): 162–164
- Hildebrand M (2003). Biological processing of nanostructured silica in diatoms. *Prog Org Coat*, 47(3–4): 256–266
- Hildebrand M (2008). Diatoms, biomineralization processes, and genomics. *Chem Rev*, 108(11): 4855–4874
- Hodge A, Petruska J (1963). *Aspects of Protein Structure*. New York: Academic Press
- Hulmes D J, Wess T J, Prockop D J, Fratzl P (1995). Radial packing, order, and disorder in collagen fibrils. *Biophys J*, 68(5): 1661–1670
- Kaluzhnaya O, Belikova A, Podolskaya E, Krasko A, Müller W, Belikov S (2007). Identification of silicateins in freshwater sponge *Lubomirskia baicalensis*. *Mol Biol*, 41(4): 554–561
- Katz E P, Li S T (1973). Structure and function of bone collagen fibrils. *J Mol Biol*, 80(1): 1–15
- Kisailus D, Truong Q, Amemiya Y, Weaver J C, Morse D E (2006). Self-assembled bifunctional surface mimics an enzymatic and templating protein for the synthesis of a metal oxide semiconductor. *Proc Natl Acad Sci USA*, 103(15): 5652–5657
- Komeili A (2007). Molecular mechanisms of magnetosome formation. *Annu Rev Biochem*, 76(1): 351–366
- Komeili A (2012). Molecular mechanisms of compartmentalization and biomineralization in magnetotactic bacteria. *FEMS Microbiol Rev*, 36(1): 232–255
- Krasko A, Lorenz B, Batel R, Schröder H C, Müller I M, Müller W E G (2000). Expression of silicatein and collagen genes in the marine sponge *Suberites domuncula* is controlled by silicate and myotrophin. *Eur J Biochem*, 267(15): 4878–4887
- Krasko A, Schröder H C, Batel R, Grebenjuk V A, Steffen R, Müller I M, Müller W E G (2002). Iron induces proliferation and morphogenesis in primmorphs from the marine sponge *Suberites domuncula*. *DNA Cell Biol*, 21(1): 67–80
- Kröger N, Poulsen N (2008). Diatoms—from cell wall biogenesis to nanotechnology. *Annu Rev Genet*, 42(1): 83–107
- Landis W J, Silver F H (2009). Mineral deposition in the extracellular matrices of vertebrate tissues: identification of possible apatite nucleation sites on type I collagen. *Cells Tissues Organs*, 189(1–4): 20–24
- Levi C, Barton J L, Guillemet C, Bras E, Lehuede P (1989). A remarkably strong natural glassy rod: the anchoring spicule of the *Monorhaphis* sponge. *J Mater Sci Lett*, 8(3): 337–339
- Mahamid J, Aichmayer B, Shimoni E, Ziblat R, Li C, Siegel S, Paris O, Fratzl P, Weiner S, Addadi L (2010). Mapping amorphous calcium phosphate transformation into crystalline mineral from the cell to the bone in zebrafish fin rays. *Proc Natl Acad Sci USA*, 107(14): 6316–6321
- Matsunaga S, Sakai R, Jimbo M, Kamiya H (2007). Long-chain polyamines (LCPAs) from marine sponge: possible implication in spicule formation. *ChemBioChem*, 8(14): 1729–1735
- Matsunaga T, Okamura Y, Fukuda Y, Wahyudi A T, Murase Y, Takeyama H (2005). Complete genome sequence of the facultative anaerobic magnetotactic bacterium *Magnetospirillum* sp. strain AMB-1. *DNA Res*, 12(3): 157–166
- Miller A and Parker S B (1984). Collagen: The organic matrix of bone. *Philos Trans R Soc, B* 304(1121): 455–477

- Moradian-Oldak J (2001). Amelogenins: assembly, processing and control of crystal morphology. *Matrix Biol*, 20(5-6): 293–305
- Moradian-Oldak J, Bouropoulos N, Wang L, Gharakhanian N (2002). Analysis of self-assembly and apatite binding properties of amelogenin proteins lacking the hydrophilic C-terminal. *Matrix Biol*, 21(2): 197–205
- Moradian-Oldak J, Du C, Falini G (2006). On the formation of amelogenin microribbons. *Eur J Oral Sci*, 114(s1 Suppl 1): 289–296, discussion 327–329, 382
- Moradian-Oldak J, Jimenez I, Maltby D, Fincham A G (2001). Controlled proteolysis of amelogenins reveals exposure of both carboxy- and amino-terminal regions. *Biopolymers*, 58(7): 606–616
- Moradian-Oldak J, Paine M L, Lei Y P, Fincham A G, Snead M L (2000). Self-assembly properties of recombinant engineered amelogenin proteins analyzed by dynamic light scattering and atomic force microscopy. *J Struct Biol*, 131(1): 27–37
- Müller W E G, Boreiko A, Schlossmacher U, Wang X, Tahir M N, Tremel W, Brandt D, Kaandorp J A, Schröder H C (2007). Fractal-related assembly of the axial filament in the demosponge *Suberites domuncula*: relevance to biomineralization and the formation of biogenic silica. *Biomaterials*, 28(30): 4501–4511
- Murat D, Byrne M, Komeili A (2010a). Cell biology of prokaryotic organelles. *Cold Spring Harb Perspect Biol*, 2(10): a000422
- Murat D, Quinlan A, Vali H, Komeili A (2010b). Comprehensive genetic dissection of the magnetosome gene island reveals the step-wise assembly of a prokaryotic organelle. *Proc Natl Acad Sci USA*, 107(12): 5593–5598
- Murr M M, Morse D E (2005). Fractal intermediates in the self-assembly of silicatein filaments. *Proc Natl Acad Sci USA*, 102(33): 11657–11662
- Nies D H (2011). How iron is transported into magnetosomes. *Mol Microbiol*, 82(4): 792–796
- Nudelman F, Pieterse K, George A, Bomans P H, Friedrich H, Brylka L J, Hilbers P A, de With G, Sommerdijk N A (2010). The role of collagen in bone apatite formation in the presence of hydroxyapatite nucleation inhibitors. *Nat Mater*, 9(12): 1004–1009
- Ofer S, Nowik I, Bauminger E R, Papaefthymiou G C, Frankel R B, Blakemore R P (1984). Magnetosome dynamics in magnetotactic bacteria. *Biophys J*, 46(1): 57–64
- Olszta M J, Cheng X, Jee S S, Kumar R, Kim Y-Y, Kaufman M J, Douglas E P and Gower L B (2007). Bone structure and formation: A new perspective. *Mater Sci Eng, R* 58(3–5): 77–116
- Pascal J L, Clementine G, Jacques L, Thibaud C (2005). Mimicking biogenic silica nanostructures formation. *Curr Nanosci*, 1(1): 73–83
- Penninga I, de Waard H, Moskowitz B M, Bazylinski D A, Frankel R B (1995). Remanence measurements on individual magnetotactic bacteria using a pulsed magnetic field. *J Magn Magn Mater*, 149(3): 279–286
- Piez K A (1965). Characterization of a collagen from codfish skin containing three chromatographically different α chains. *Biochemistry*, 4(12): 2590–2596
- Piez K A, Lewis M S, Martin G R, Gross J (1961). Subunits of the collagen molecule. *Biochim Biophys Acta*, 53(3): 596–598
- Posner A S, Betts F (1975). Synthetic amorphous calcium phosphate and its relation to bone mineral structure. *Acc Chem Res*, 8(8): 273–281
- Pozzolini M, Sturla L, Cerrano C, Bavestrello G, Camardella L, Parodi A M, Raheli F, Benatti U, Müller W E G, Giovine M (2004). Molecular cloning of silicatein gene from marine sponge *Petrosia ficiformis* (Porifera, Demospongiae) and development of primmorphs as a model for biosilicification studies. *Mar Biotechnol* (NY), 6(6): 594–603
- Prozorov T, Mallapragada S, Narasimhan B, Wang L, Palo P, Nilsen-Hamilton M, Williams T, Bazylinski D, Prozorov R, Canfield P (2007a). Protein-mediated synthesis of uniform superparamagnetic magnetite nanocrystals. *Adv Funct Mater*, 17(6): 951–957
- Prozorov T, Palo P, Wang L, Nilsen-Hamilton M, Jones D, Orr D, Mallapragada S K, Narasimhan B, Canfield P C, Prozorov R (2007b). Cobalt ferrite nanocrystals: out-performing magnetotactic bacteria. *ACS Nano*, 1(3): 228–233
- Rabuffetti F A, Lee J S, Brutchey R L (2012). Vapor diffusion sol-gel synthesis of fluorescent perovskite oxide nanocrystals. *Adv Mater*, 24(11): 1434–1438
- Ramachandran G N, Kartha G (1955). Structure of collagen. *Nature*, 176(4482): 593–595
- Rich A, Crick F H C (1955). The structure of collagen. *Nature*, 176(4489): 915–916
- Richter M, Kube M, Bazylinski D A, Lombardot T, Glöckner F O, Reinhardt R, Schüler D (2007). Comparative genome analysis of four magnetotactic bacteria reveals a complex set of group-specific genes implicated in magnetosome biomineralization and function. *J Bacteriol*, 189(13): 4899–4910
- Schröder H C, Perović-Ottstadt S, Rothenberger M, Wiens M, Schwertner H, Batel R, Korzhev M, Müller I M, Müller W E G (2004a). Silica transport in the demosponge *Suberites domuncula*: fluorescence emission analysis using the PDMPO probe and cloning of a potential transporter. *Biochem J*, 381(Pt 3): 665–673
- Schröder H C, Perović-Ottstadt S, Wiens M, Batel R, Müller I M, Müller W E (2004b). Differentiation capacity of epithelial cells in the sponge *Suberites domuncula*. *Cell Tissue Res*, 316(2): 271–280
- Schüler D (2008). Genetics and cell biology of magnetosome formation in magnetotactic bacteria. *FEMS Microbiol Rev*, 32(4): 654–672
- Shaw W J, Campbell A A, Paine M L, Snead M L (2004). The COOH terminus of the amelogenin, LRAP, is oriented next to the hydroxyapatite surface. *J Biol Chem*, 279(39): 40263–40266
- Shimizu K, Cha J, Stucky G D, Morse D E (1998). Silicatein α : cathepsin L-like protein in sponge biosilica. *Proc Natl Acad Sci USA*, 95(11): 6234–6238
- Simmer J P, Fincham A G (1995). Molecular mechanisms of dental enamel formation. *Crit Rev Oral Biol Med*, 6(2): 84–108
- Simpson T L (1984). *The cell biology of sponges*. New York: Springer Publishing
- Staniland S, Ward B, Harrison A, van der Laan G, Telling N (2007). Rapid magnetosome formation shown by real-time X-ray magnetic circular dichroism. *Proc Natl Acad Sci USA*, 104(49): 19524–19528
- Stöber W, Fink A, Bohn E (1968). Controlled growth of monodisperse silica spheres in the micron size range. *J Colloid Interface Sci*, 26(1): 62–69
- Sumper M, Brunner E (2006). Learning from diatoms: Nature's tools for the production of nanostructured silica. *Adv Funct Mater*, 16(1): 17–26
- Tacke R (1999). Milestones in the biochemistry of silicon: From basic research to biotechnological applications. *Angew Chem Int Ed Engl*, 38(20): 3015–3018

- Tanaka M, Mazuyama E, Arakaki A, Matsunaga T (2011). MMS6 protein regulates crystal morphology during nano-sized magnetite biomineralization *in vivo*. *J Biol Chem*, 286(8): 6386–6392
- Tarasevich B J, Lea S, Bernt W, Engelhard M, Shaw W J (2009). Adsorption of amelogenin onto self-assembled and fluoroapatite surfaces. *J Phys Chem B*, 113(7): 1833–1842
- Tarasevich B J, Lea S, Shaw W J (2010). The leucine rich amelogenin protein (LRAP) adsorbs as monomers or dimers onto surfaces. *J Struct Biol*, 169(3): 266–276
- Termine J D, Kleinman H K, Whitson S W, Conn K M, McGarvey M L, Martin G R (1981). Osteonectin, a bone-specific protein linking mineral to collagen. *Cell*, 26(1 Pt 1): 99–105
- Termine J D, Posner A S (1966). Infrared analysis of rat bone: age dependency of amorphous and crystalline mineral fractions. *Science*, 153(3743): 1523–1525
- Thiel P A, Shen M, Liu D J, Evans J W (2009). Coarsening of two-dimensional nanoclusters on metal surfaces. *J Phys Chem C*, 113(13): 5047–5067
- Traub W, Arad T, Weiner S (1989). Three-dimensional ordered distribution of crystals in turkey tendon collagen fibers. *Proc Natl Acad Sci USA*, 86(24): 9822–9826
- Uebe R, Junge K, Henn V, Poxleitner G, Katzmann E, Plitzko J M, Zarivach R, Kasama T, Wanner G, Pósfai M, Böttger L, Matzanke B, Schüler D (2011). The cation diffusion facilitator proteins MamB and MamM of *Magnetospirillum gryphiswaldense* have distinct and complex functions, and are involved in magnetite biomineralization and magnetosome membrane assembly. *Mol Microbiol*, 82(4): 818–835
- Wang L, Prozorov T, Palo P E, Liu X, Vaknin D, Prozorov R, Mallapragada S, Nilsen-Hamilton M (2012a). Self-assembly and biphasic iron-binding characteristics of Mms6, a bacterial protein that promotes the formation of superparamagnetic magnetite nanoparticles of uniform size and shape. *Biomacromolecules*, 13(1): 98–105
- Wang W, Bu W, Wang L, Palo P E, Mallapragada S, Nilsen-Hamilton M, Vaknin D (2012b). Interfacial properties and iron binding to bacterial proteins that promote the growth of magnetite nanocrystals: X-ray reflectivity and surface spectroscopy studies. *Langmuir*, 28(9): 4274–4282
- Weaver J C, Morse D E (2003). Molecular biology of demosponge axial filaments and their roles in biosilicification. *Microsc Res Tech*, 62(4): 356–367
- Weiner S (2006). Transient precursor strategy in mineral formation of bone. *Bone*, 39(3): 431–433
- Weiner S (2008). Biomineralization: a structural perspective. *J Struct Biol*, 163(3): 229–234
- Weiner S, Addadi L (1991). Acidic macromolecules of mineralized tissues: the controllers of crystal formation. *Trends Biochem Sci*, 16(7): 252–256
- Wheeler E J, Lewis D (1977). An x-ray study of the paracrystalline nature of bone apatite. *Calcif Tissue Res*, 24(3): 243–248
- Yuk J M, Park J, Ercius P, Kim K, Hellebusch D J, Crommie M F, Lee J Y, Zettl A, Alivisatos A P (2012). High-resolution EM of colloidal nanocrystal growth using graphene liquid cells. *Science*, 336(6077): 61–64
- Zeichner-David M, Diekwisch T, Fincham A, Lau E, MacDougall M, Moradian-Oldak J, Simmer J, Snead M, Slavkin H C (1995). Control of ameloblast differentiation. *Int J Dev Biol*, 39(1): 69–92
- Zhou Y, Shimizu K, Cha J N, Stucky G D, Morse D E (1999). Efficient catalysis of polysiloxane synthesis by silicatein α requires specific hydroxy and imidazole functionalities. *Angew Chem Int Ed Engl*, 38(6): 779–782